Applied Nanoscience (2020) 10:3133–3141
https://doi.org/10.1007/s13204-019-01052-y

ORIGINAL ARTICLE

Chemically reactive and nonlinear radiative heat flux in mixed convection flow of Oldroyd-B nanofluid

M. Irfan[1] · M. Khan[1] · M. Mudassar Gulzar[2] · W. A. Khan[3]

Received: 31 January 2019 / Accepted: 4 May 2019 / Published online: 24 May 2019

Abstract
This paper investigates the aspects of magnetic field and chemical reaction in Oldroyd-B nanofluid influenced by a stretching cylinder. The properties of mixed convection, nonlinear radiation and heat sink/source are incorporated. By means of noteworthy conversions, the nonlinear PDEs are altered into nonlinear ODEs and elucidated via homotopic approach. The influence of countless variables for velocity, temperature and concentration fields in addition to local Nusselt and Sherwood numbers are portrayed and conferred. These upshots portray that the liquid velocity enhances for intensifying value of mixed convection parameter whereas, it diminish for magnetic parameter. Moreover, the Brownian motion parameter and radiation parameter enhances the liquid temperature of Oldroyd-B nanofluid. For the endorsement of current upshots an assessment values in restrictive circumstances is also presented.

Keywords Oldroyd-B nanofluid · Mixed convection · Nonlinear thermal radiation · Heat sink/source · Chemical reaction

Introduction

At present, the thoughtfulness of nanomaterial's has increased noteworthy reputation from the researchers and scientists. Limited thermal aspects of established liquids confine their suitability for up-to-date utilizations demanding a high level enactment, while retaining compact size of the thermal structures. For instance, micro-electromechanical systems and make cold of chips in computer mainframes and to acquire fast transient systems in warming structures. Nanoliquids are diluted deferral of nano-scale elements in disreputable liquids which exaggerates the heat transfer of the elucidation and intensify the storage propensity. Nanofluids have engrossing thermo-physical aspects and heat transfer enactment with energetic probable uses owing to which these are deliberated as next generation heat transport liquids. The hybrid-powered procedures, solar accumulators, engine and energy cells, pharmacological development and atomic uses are specimens of developing nanotechnologies. The notion to intensifying the thermal conductivity of disreputable liquids was presented by Choi (1995). Later on, numerous theoretical and experimental exertions are established to scrutinize the diverse aspects of nanofluids see (Mustafa et al. 2015; Mahanthesh et al. 2016, 2017a, b; Hayat et al. 2017a, b; Anwar and Rasheed 2017; Haq et al. 2017; Khan et al. 2017). Numerically a reviewed model for MHD flow of Carreau nanomaterial was considered by Waqas et al. (2017a). Their study established that radiation parameter and Biot number enhanced the liquid temperature of Carreau nanofluid. By exploiting the approach of CVFEM, Sheikholeslami and Oztop (2017) reported the aspect of MHD in Fe_3O_4-water nanoliquid in a cavity with sinusoidal outside cylinder. Aspects of chemical reaction and MHD in 3D radiative flow of nanofluid were considered by Hayat et al. (2018). They noted that the nanoparticles volume fraction and magnetic parameter rises the skin friction coefficient. The properties of the heat sink/source and convective heat transport in Maxwell nanomaterial was explored by Irfan et al. (2018). They acquired that the liquid velocity decays for magnetic parameter and intensified the temperature and concentration fields. Recently, Ellahi (2018) disclosed the modern advances of nanoliquids. He reported that nanofluid technology can

✉ M. Irfan
mirfan@math.qau.edu.pk

1 Department of Mathematics, Quaid-i-Azam University, Islamabad 44000, Pakistan

2 National University of Technology, Sector I-12, Islamabad 44000, Pakistan

3 Department of Mathematics, Mohi-Ud-Din Islamic University Nerian Sharif, Azad Jammu and Kashmir, Pakistan

benefit to improve superior emollients and oils for real-world solicitations. Haq et al. (2019) reported the behavior of thermal management of carbon nanotubes in partially heated triangular cavity. Sheikholeslami et al. (2019) studied the aspect of heat transport by heat storage unit utilizing nanoparticles.

No doubt the behavior of chemical reaction spectacles enthusiastic parts with the intention to scrutinize the aspects of heat and mass transport in built-up regions. Utilizations of a chemical reaction can initiate in diverse industrial and built-up uses for that instance, solar antenna, the strategy of chemical dispensation apparatus, rubbery isolation, dispersion of prescription in lifeblood, effluence, humidity over gardening pitches and fissionable discarded depositories etc. Furthermore, the first order chemical reaction is directly correlated to the concentration and numerous studies on chemical reaction with diverse geometries can be comprehended in Anjalidevi and Kandasamy (1999), Zhang et al. (2015), Hayat et al. (2017c), Kumar et al. (2017). Sreedevi et al. (2017) presented chemically radiated nanofluid in porous media by functioning numerical Galerkin (FEM) approach. Hayat et al. (2017c) studied the performance of chemical reaction and nonlinear thermal radiation in magneto Jeffrey liquid considering Newtonian heating. Their analysis established conflicted behavior for destructive and generative chemical reaction parameter on concentration field. Alshomrani et al. (2018) scrutinized the combined aspects of stratifications and convective phenomena in chemically reactive Oldroyd-B fluid. The thermal radiation and MHD impacts were also presented. Their assessment reported that the reaction parameter and mass Biot number decline the concentration field. Aspects of chemical reaction and non-Fourier heat flux theory in Carreau nanoliquid with wedge and cone geometries have been reported by Kumar et al. (2018). They established that the features of flow and transfer were controlled when nanoparticle volume fraction varies. The characteristics of chemical reaction in radiated flow of Maxwell nanofluid caused by rotating disk were examined by Ahmed et al. (2019).

Here our strategic concern is to scrutinize the aspects of MHD mixed convection in nonlinear radiative Oldroyd-B fluid. The impact of heat sink/source and chemical reaction are also considered. Elucidations are established through homotopic scheme (Rehman et al. 2017; Irfan et al. 2019a, b; Rashid et al. 2019). To confer the somatic performance of emerging variables graphs are portrayed. Endorsement of the current analytical process is made by associating the outcomes of $-f''(0)$ with presented studies and such assessment seems to be worthy in agreement.

Development of mathematical model

Here we analyze steady ($2D$) MHD flow of Oldroyd-B fluid caused by stretching cylinder of radius R with velocity $\frac{U_0 z}{l}$ along z-directions, where (U_0, l) represents reference velocity and specific length, respectively. Furthermore, the aspects of mixed convection, nonlinear radiation, heat sink/source and chemical reaction are reported. Consider the cylindrical polar coordinates (z, r) in such scheme that z-axis goes close to the axis of the cylinder and r-axis is restrained near the radial direction. We consider electrically conducting fluid where applied magnetic field acts transversely to the flow. The influence of induced magnetic field on Oldroyd-B fluid is neglected because of small Reynolds number. Additionally, the flow field is effected by magnetic strength B_0 (see Fig. 1).

The equations of Oldroyd-B nanofluid under these norms can be written as (Irfan et al. 2019a, b):

$$\frac{\partial u}{\partial r} + \frac{u}{r} + \frac{\partial w}{\partial z} = 0, \tag{1}$$

$$\begin{aligned} u\frac{\partial w}{\partial r} + w\frac{\partial w}{\partial z} + \lambda_1\left[w^2\frac{\partial^2 w}{\partial z^2} + u^2\frac{\partial^2 w}{\partial r^2} + 2uw\frac{\partial^2 w}{\partial r\partial z}\right] \\ = \upsilon\left[\frac{\partial^2 w}{\partial r^2} + \frac{1}{r}\frac{\partial w}{\partial r}\right] + \upsilon\lambda_2\left[\frac{u}{r^2}\frac{\partial w}{\partial r} - \frac{1}{r}\frac{\partial w}{\partial r}\frac{\partial w}{\partial z}\right. \\ -\frac{2}{r}\frac{\partial u}{\partial r}\frac{\partial w}{\partial r} + \frac{w}{r}\frac{\partial^2 w}{\partial r\partial z} - \frac{\partial w}{\partial r}\frac{\partial^2 w}{\partial r\partial z} - 2\frac{\partial w}{\partial r}\frac{\partial^2 u}{\partial r^2} \\ \left.+\frac{u}{r}\frac{\partial^2 w}{\partial r^2} - \frac{\partial w}{\partial z}\frac{\partial^2 w}{\partial r^2} - w\frac{\partial^3 w}{\partial r^2\partial z} + u\frac{\partial^3 w}{\partial r^3}\right] \\ - \frac{\sigma B_0^2}{\rho_f}\left(w + \lambda_1 u\frac{\partial w}{\partial r}\right) + g[\beta_T(T - T_\infty) + \beta_C(C - C_\infty)], \end{aligned} \tag{2}$$

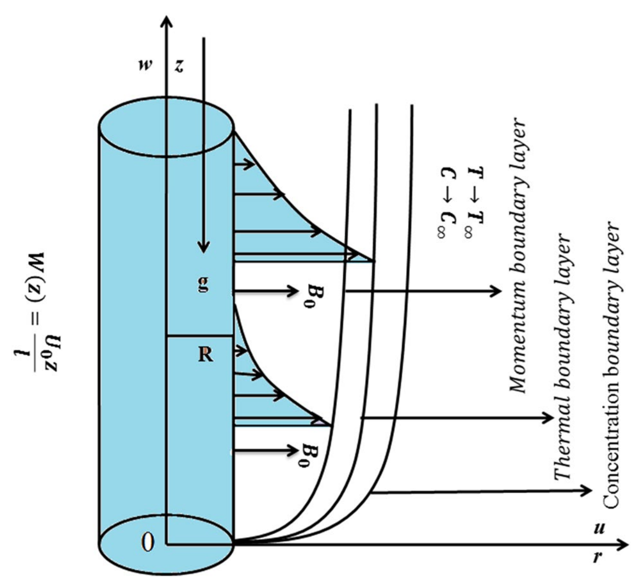

Fig. 1 Flow configuration and coordinates system

$$u\frac{\partial T}{\partial r}+w\frac{\partial T}{\partial z}=\alpha_1\left[\frac{\partial^2 T}{\partial r^2}+\frac{1}{r}\frac{\partial T}{\partial r}\right]+\tau\left[D_B\frac{\partial C}{\partial r}\frac{\partial T}{\partial r}+\frac{D_T}{T_\infty}\left(\frac{\partial T}{\partial r}\right)^2\right]-\frac{1}{(\rho c)_f}\frac{1}{r}\frac{\partial(rq_r)}{\partial r}-\frac{Q_0(T-T_\infty)}{(\rho c)_f},\tag{3}$$

$$u\frac{\partial C}{\partial r}+w\frac{\partial C}{\partial z}=D_B\frac{1}{r}\frac{\partial}{\partial r}\left[\left(r\frac{\partial C}{\partial r}\right)\right]+\frac{D_T}{T_\infty}\frac{1}{r}\frac{\partial}{\partial r}\left[\left(r\frac{\partial T}{\partial r}\right)\right]-k_c(C-C_\infty),\tag{4}$$

with boundary conditions

$$w(r,z)=W(z)=\frac{U_0 z}{l},\quad u(r,z)=0,$$
$$T=T_w,\quad C=C_w,\quad \text{at}\quad r=R,\tag{5}$$

$$w\to 0,\quad T\to T_\infty,\quad C\to C_\infty\quad \text{at}\quad r\to\infty.\tag{6}$$

Here (u, w) signify the velocity components in r- and z-directions, respectively, $\lambda_i\,(i=1,\,2)$ the relaxation–retardation times, respectively, ν the kinematic viscosity, σ the nanofluid electrically conductivity, g the gravitational acceleration, (β_T, β_C) are the thermal and concentration expansion coefficients, respectively, α_1 the thermal diffusivity of nanoliquid, (ρ_f, c_f) the liquid density and specific heat, respectively, (T, C) the temperature and concentration of nanoliquid, respectively, τ the ratio of effective heat capacity of nanomaterial to the heat capacity of the base liquid, (D_B, D_T) the Brownian and thermophoresis diffusion coefficients, respectively, (T_∞, C_∞) the temperature and concentration of nanoliquid far-off from the stretched surface, Q_0 the heat sink/source coefficient and k_c the reaction rate. Furthermore, via Rossland's approximation the nonlinear radiative heat flux q_r is given as

$$q_r=-\frac{4\sigma^*}{3k^*}\frac{\partial T^4}{\partial r}=-\frac{16\sigma^*}{3k^*}T^3\frac{\partial T}{\partial r},\tag{7}$$

where (σ^*, k^*) are the Stefan Boltzmann constant and the mean absorption coefficient, respectively.

Appropriate transformations

Let us consider

$$u=-\frac{R}{r}\sqrt{\frac{U_0\nu}{l}}f(\eta),\quad w=\frac{U_0 z}{l}f'(\eta),\quad \eta=\sqrt{\frac{U_0}{\nu l}}\left(\frac{r^2-R^2}{2R}\right),$$
$$\theta(\eta)=\frac{T-T_\infty}{T_w-T_\infty},\quad \varphi(\eta)=\frac{C-C_\infty}{C_w-C_\infty}.\tag{8}$$

Using Eqs. (7) and (8), then Eqs. (1)–(6) reduced to

$$(1+2\alpha\eta)f'''+2\alpha f''+ff''-f'^2+2\beta_1 ff'f''-\beta_1 f^2f'''-\frac{\alpha\beta_1}{(1+2\alpha\eta)}f^2f''+(1+2\alpha\eta)\beta_2(f''^2-ff^{iv})-4\alpha\beta_2 ff'''-M^2(f'-\beta_1 ff'')+\lambda(\theta+N\varphi)=0,\tag{9}$$

$$[\{1+R_d(1+(\theta_w-1)\theta)^3\}(1+2\alpha\eta)\theta']'+Prf\theta'+(1+2\alpha\eta)\Pr N_b\theta'\varphi'+(1+2\alpha\eta)Pr\,N_t\theta'^2+Pr\,\delta\theta=0,\tag{10}$$

$$(1+2\alpha\eta)\varphi''+2\alpha\varphi'+LePrf\,\varphi'+(1+2\alpha\eta)\left(\frac{N_t}{N_b}\right)\theta''+2\alpha\left(\frac{N_t}{N_b}\right)\theta'-Le\,Pr\,C_r\varphi=0,\tag{11}$$

$$f(0)=0,\quad f'(0)=1,\quad \theta(0)=1,\quad \varphi(0)=1,\tag{12}$$

$$f'(\infty)=0,\quad \theta(\infty)=0,\quad \varphi(\infty)=0.\tag{13}$$

Here $\alpha=\left(\frac{1}{R}\sqrt{\frac{\nu l}{U_0}}\right)$ the curvature parameter, $\beta_i=\left(\frac{\lambda_i U_0}{l}\right)(i=1,2)$ Deborah numbers, $M=\left(\sqrt{\frac{\sigma l B_0^2}{U_0\rho_f}}\right)$ magnetic parameter, $\lambda=\left(\frac{g\beta_T(T_w-T_\infty)}{U_0^2 z}\right)$ mixed convection parameter, $N=\left(\frac{\beta_C(C_w-C_\infty)}{\beta_T(T_w-T_\infty)}\right)$ buoyancy parameter, $R_d=\left(\frac{16\sigma^* T_\infty^3}{3kk^*}\right)$ Radiation parameter, $\theta_w=\left(\frac{T_w}{T_\infty}\right)$ temperature ratio parameter, $Pr=\left(\frac{\nu}{\alpha_1}\right)$ Prandtl number, $N_b=\left(\frac{\tau D_B(C_w-C_\infty)}{\nu}\right)$ Brownian motion parameter, $N_t=\left(\frac{\tau D_T(T_w-T_\infty)}{\nu T_\infty}\right)$ thermophoresis parameter, $Le=\left(\frac{\alpha_1}{D_B}\right)$ Lewis number and $C_r=\left(\frac{k_c l}{U_0}\right)$ chemical reaction parameter.

Physical quantities of notable interest

The industrial point of vision the quantities of physical interest are the local Nusselt and local Sherwood numbers, respectively.

The local Nusselt and Sherwood numbers

The local Nusselt and Sherwood numbers are defined by

$$Nu_z=\frac{zq_m}{k(T_w-T_\infty)},\quad Sh_z=\frac{zj_m}{D_B(C_w-C_\infty)},\tag{14}$$

where q_m the heat flux and j_m the mass flux, respectively, and defined as

$$q_w=-k\left(\frac{\partial T}{\partial r}\right)_{r=R}-\frac{16\sigma^* T^3}{3k^*}\left(\frac{\partial T}{\partial r}\right)_{r=R},\quad j_m=-D_B\left(\frac{\partial C}{\partial r}\right)_{r=R},\tag{15}$$

The dimensionless quantities are

$$Nu_zRe_z^{-\frac{1}{2}}=-\left(1+\frac{4}{3}R_d\left(1+\left(\theta_w-1\right)\theta(0)\right)\right)^3\theta'(0),$$
$$Sh_zRe_z^{-\frac{1}{2}}=-\varphi'(0).\tag{16}$$

where $Re_z = \frac{W(z)z}{v}$ signifies the local Reynolds number.

Solution methodology

Homotopy analysis solutions (HAM)

The nonlinear ODEs (9)–(11) with boundary conditions (12) and (13) are elucidated via homotopic algorithm (HAM). The initial guesses $(f_0, \theta_0, \varphi_0)$ and auxiliary linear operators $(L_f, L_\theta, L_\varphi)$ are defined as:

$$f_0(\eta) = 1 - \exp(-\eta), \quad \theta_0(\eta) = \exp(-\eta), \quad \varphi_0(\eta) = \exp(-\eta), \tag{17}$$

$$L_f = \frac{d^3 f}{d\eta^3} - \frac{df}{d\eta}, \quad L_\theta = \frac{d^2\theta}{d\eta^2} - \theta, \quad L_\varphi = \frac{d^2\varphi}{d\eta^2} - \varphi, \tag{18}$$

The overhead operators satisfied the following properties

$$\begin{aligned} &L_f\left[C_1^* + C_2^* \exp(\eta) + C_3^* \exp(-\eta)\right] = 0,\\ &L_\theta\left[C_4^* \exp(\eta) + C_5^* \exp(-\eta)\right] = 0,\\ &L_\varphi\left[C_6^* \exp(\eta) + C_7^* \exp(-\eta)\right] = 0, \end{aligned} \tag{19}$$

here $C_i^*(i = 1\text{–}7)$ are the arbitrary constants.

Analysis

The aspects of influential parameters on velocity $f'(\eta)$, temperature $\theta(\eta)$, concentration $\varphi(\eta)$ and Nusselt number $Nu_z Re_z^{-\frac{1}{2}}$ are highlighted in this section. The homotopic methodology has been utilized. The executed values of influential parameters throughout the computations are $\beta_1 = \beta_2 = N = \lambda = N_t = C_r = 0.2$, $\alpha = N_b = \delta = 0.3$, $M = 0.4$, $R_d = 0.5$, $Pr = \theta_w = 1.2$ and $Le = 1$ except particular pointed out in the graphs. Additionally, the assessment of $-f''(0)$ for different values of β_1 with former attainable studies are reported in Table 1. An admirable settlement is being established from this table which satisfies us that our outcomes are accurate.

Velocity $f'(\eta)$

On velocity field $f'(\eta)$ the aspects of magnetic parameter (M) and mixed convection parameter (λ) are plotted which are exposed in Fig. 2a, b. The velocity field decline for M; however, rise for λ when the values of these parameter enhanced. The Lorentz force intensifies, when we heighten M, which formed more struggle to the fluid motion. Therefore, velocity of Oldroyd-B fluid falloffs. Moreover, physically buoyancy force goes as boosting pressure gradient, so stronger buoyancy force helps the flow in the growing direction which enhance $f'(\eta)$ when λ enlarged.

Temperature $\theta(\eta)$

The aspects of curvature parameter (α) and Deborah number (β_2) on temperature field $\theta(\eta)$ are established in Fig. 3a, b. The higher value of α enhances the temperature of Oldroyd-B fluid; however, conflicting behavior is being noted for β_2. The increasing values of α decline the heat transfer quantity, which enhances the temperature field. Moreover, physically, β_2 involves retardation time, which causes a reduced in temperature for larger retardation time and hence, the temperature field decreases. The Brownian (N_b) and thermophoretic (N_t) nanoparticles impact on temperature field $\theta(\eta)$ is reported in Fig. 4a, b. The temperature field decline for higher N_b and similar enactment is being remarked for N_t. As, Brownian motion is an unsystematic exertion of liquid particles, which molded much heat to the liquid and enhances the temperature field. Similar portrayal for larger N_t is true on temperature field which intensifies the temperature of Oldroyd-B fluid. Figure 5a, b discussed the physical aspects of thermal radiation (R_d) and magnetic parameter (M) on temperature field. Both the parameters are intensifying function of temperature field, when R_d and M enlarged. As we increase R_d the mean absorption coefficient declines and thermal thickness of the layer uninterruptedly

Table 1 A comparison of β_1 for $-f''(0)$ in limiting sense when $\beta_2 = M = \lambda = N = 0$

$-f''(0)$					
β_1	Abel et al. (2012)	Meghed (2013)	Waqas et al. (2017b)	Irfan et al. (2018)	Present
.0	1.000000	0.999978	1.000000	1.0000000	1.0000000
0.2	1.051948	1.051945	1.051889	1.0518899	1.0518899
0.4	1.101850	1.101848	1.101903	1.1019033	1.1019032
0.6	1.150163	1.150160	1.150137	1.1501373	1.1501373
0.8	1.196692	1.196690	1.196711	1.1967113	1.1967113
1.2	1.285257	1.285253	1.285363	1.2853632	1.2853632
1.6	1.368641	1.368641	1.368758	1.3687584	1.3687584
2.0	1.447617	1.447616	1.447651	1.4476527	1.4476527

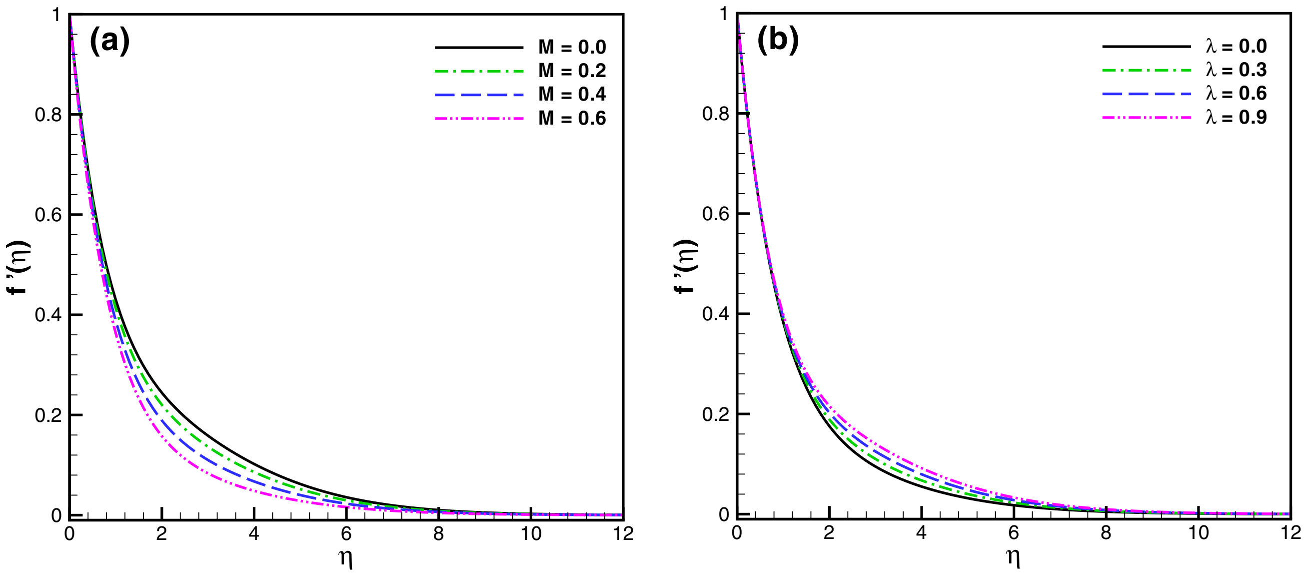

Fig. 2 Impact of **a** M and **b** λ on $f'(\eta)$

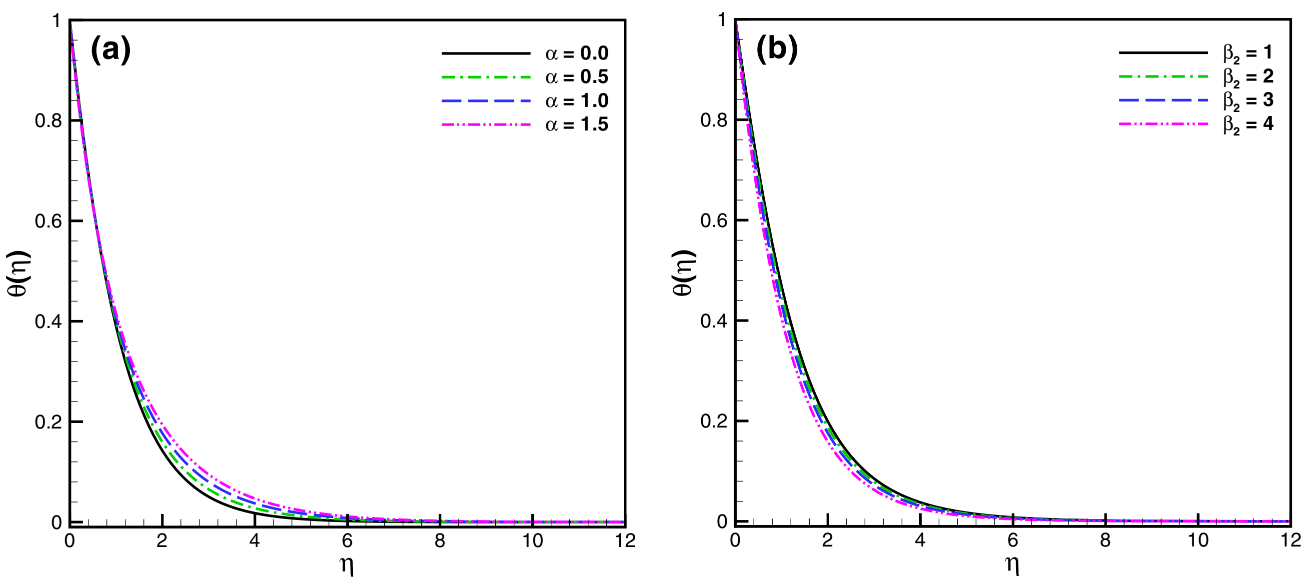

Fig. 3 Impact of **a** α and **b** β_2 on $\theta(\eta)$

intensifies. Hence, temperature field for R_d escalates. Furthermore, the higher M spectacles identical performance on temperature field. The Lorentz force is a resistive force and M is related to Lorentz force. The enhancing in M transport extra effort which exaggerates temperature field. The temperature field of Oldroyd-B nanofluid for heat sink/source parameter (δ) is plotted in Fig. 6a, b. These strategies recognize conflicting enactment on temperature field. The huge quantity of heat is fascinated for ($\delta < 0$) and enormous amount of heat is provided ($\delta > 0$), respectively, to the fluid when we intensified these parameters. This reason causes the decay of temperature field for ($\delta < 0$); however, conflicting enactment is acknowledge for ($\delta > 0$).

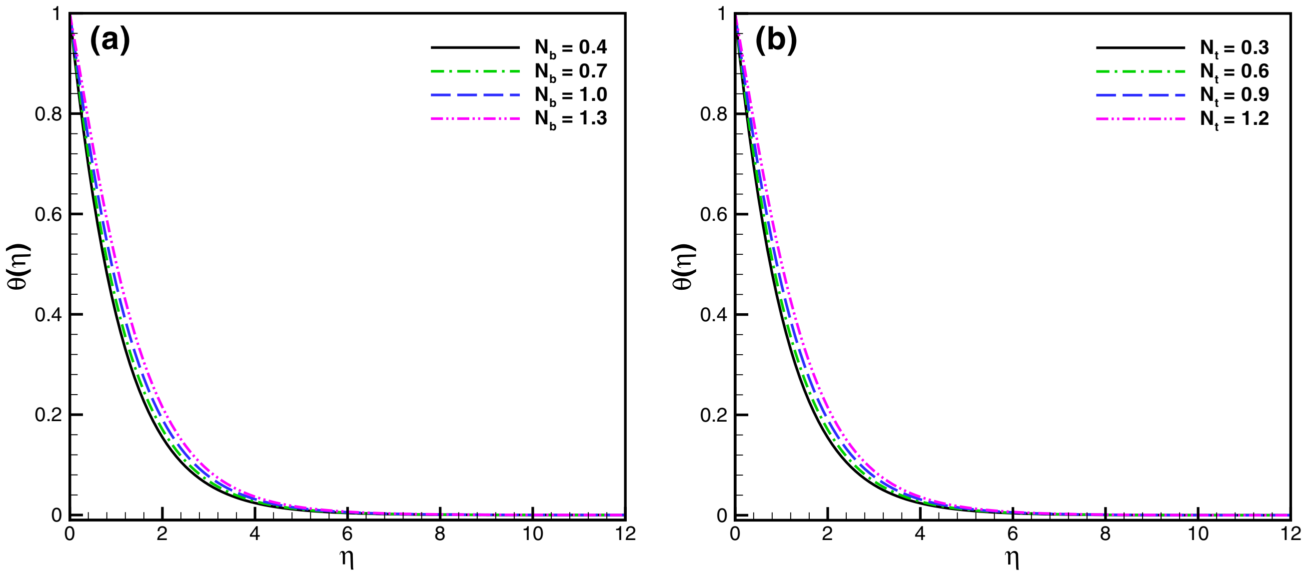

Fig. 4 Impact of **a** N_b and **b** N_t on $\theta(\eta)$

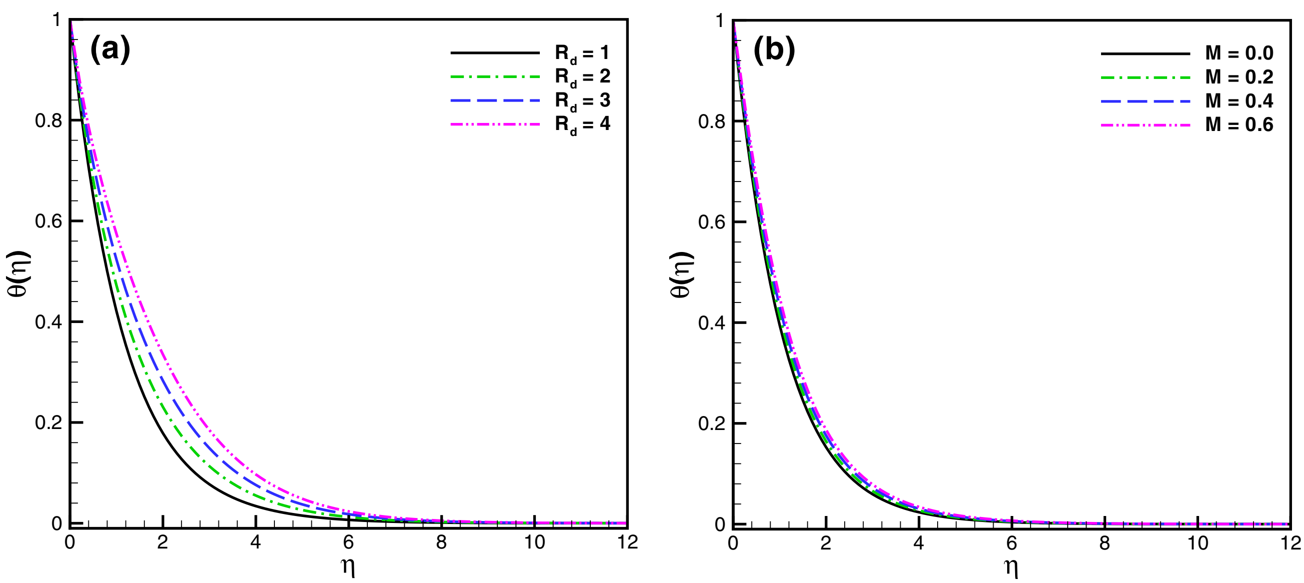

Fig. 5 Impact of **a** R_d and **b** M on $\theta(\eta)$

Concentration field $\varphi(\eta)$

To establish the properties of reaction parameter (C_r) and Lewis number (Le) on the concentration field Fig. 7a, b is depicted. These diagrams exhibit analogous enactment and decline the concentration field. For larger value of C_r exaggerates the quantity of chemical reaction and liquid species more proficiently, which decays concentration field. Moreover, same trend is noted for Le on concentration field for augmented values of Le. In conclusion, we reported that both C_r and Le have identical impact on Oldroyd-B concentration field.

Local Nusselt number $Nu_z Re_z^{-\frac{1}{2}}$

Figures 8a, b and 9a, b are acknowledged to plot the aspects of influential parameters on Nusselt number for the fluctuating values of N_b, N_t, R_d and Pr. These depictions reported that the heat transport amount decays for the higher values of these parameters.

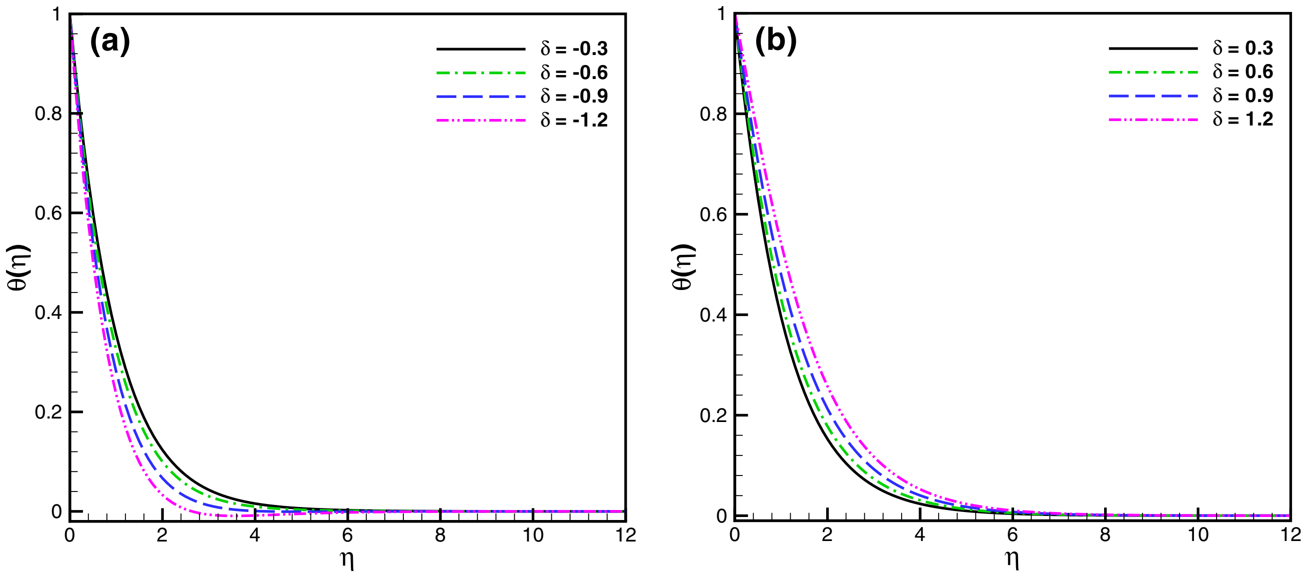

Fig. 6 Impact of **a** $\delta < 0$ and **b** $\delta > 0$ on $\theta(\eta)$

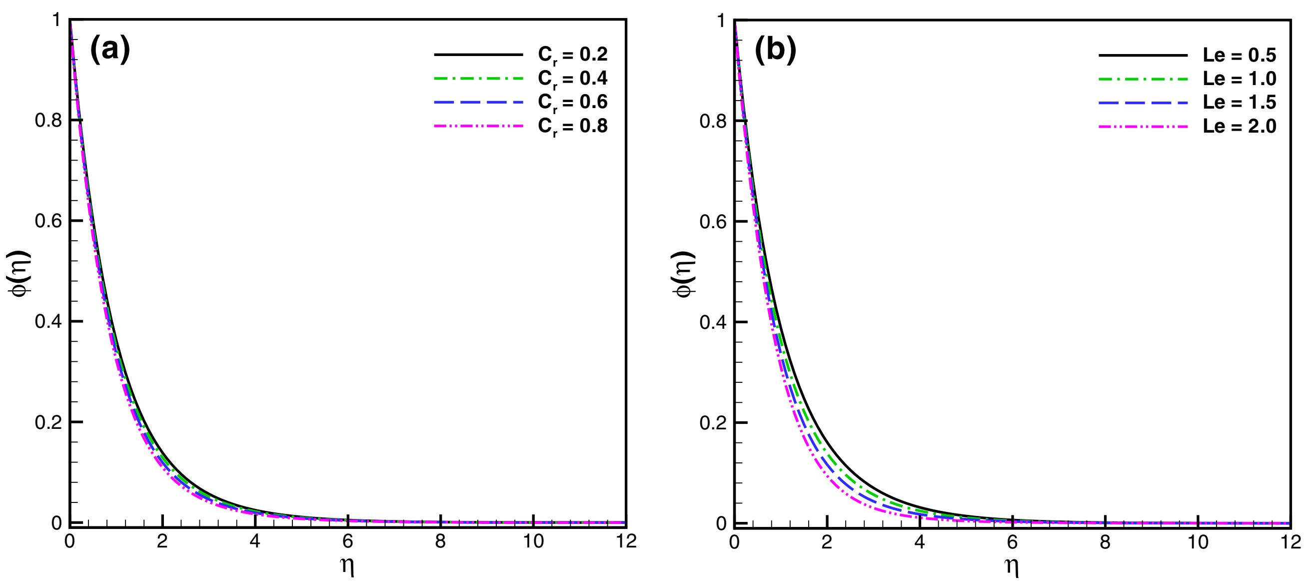

Fig. 7 Impact of **a** C_r and **b** Le on $\varphi(\eta)$

Closing remarks

The nonlinear aspects of thermal radiation subject to chemical reaction in flow of an Oldroyd-B nanofluid with magnetic and mixed convection properties were studied. The heat sink/source features were also incorporated. The essential conclusions of this study itemized below:

- The higher values of M declined the velocity field; however, for λ the velocity of Oldroyd-B fluid enhanced.
- Opposed behavior were noted for larger α and β_2 on $\theta(\eta)$.
- The intensifying values of N_b and N_t boosted the temperature of Oldroyd-B fluid, while conflicted performance were reported for $\delta < 0$ and $\delta > 0$ on $\theta(\eta)$.

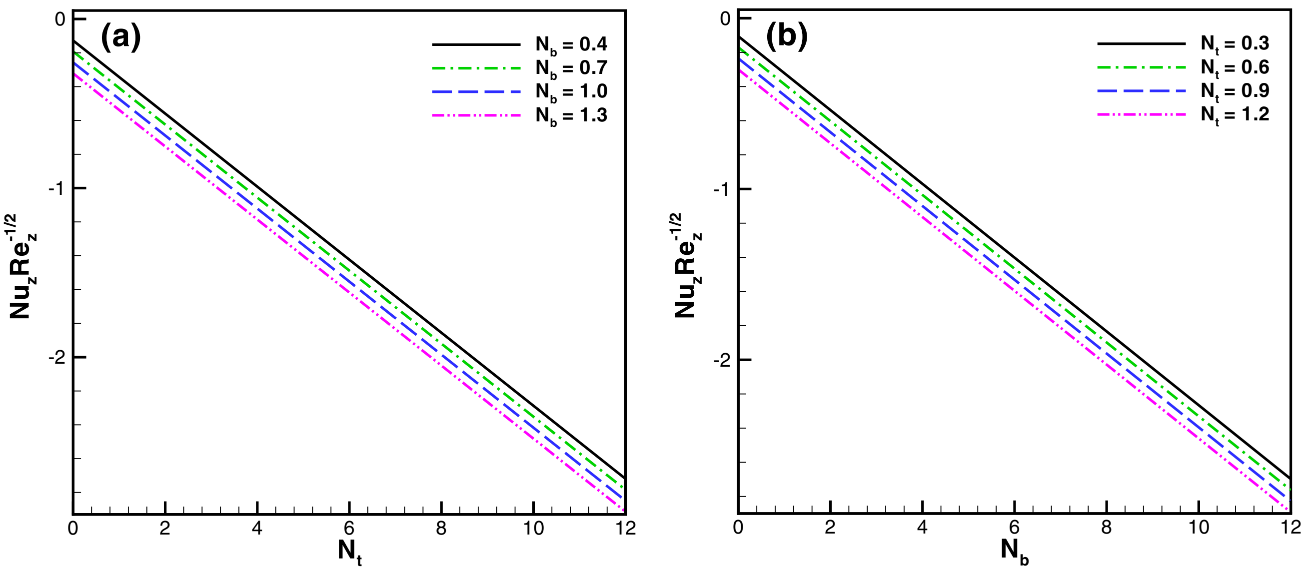

Fig. 8 Impact of **a** N_b and **b** N_t on $Nu_z Re_z^{-\frac{1}{2}}$

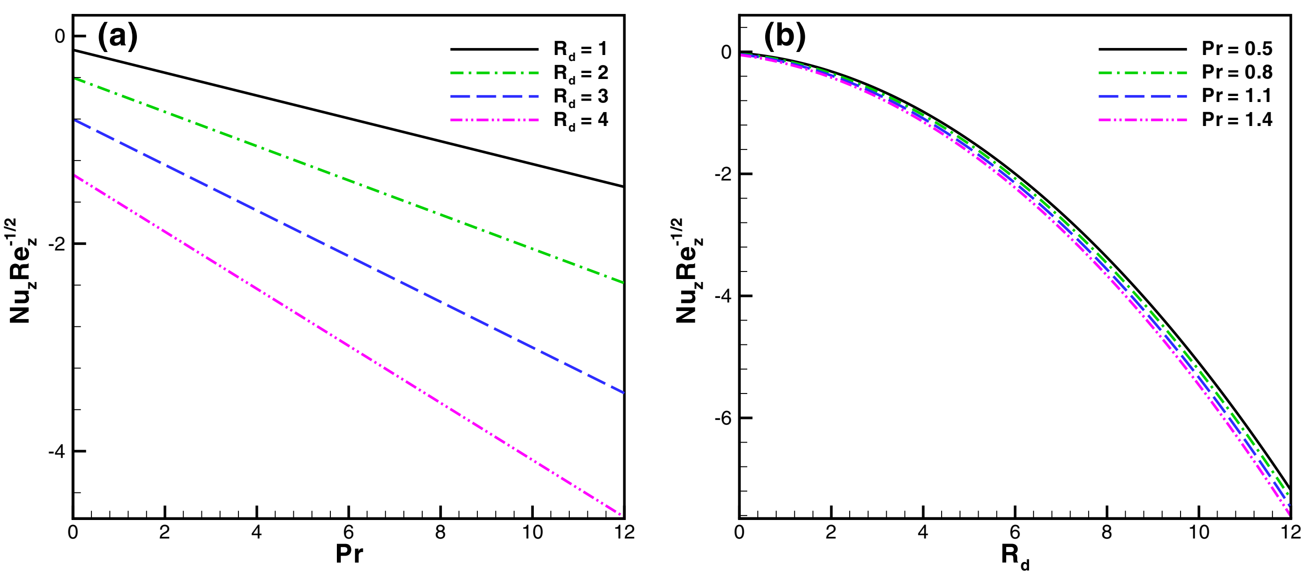

Fig. 9 Impact of **a** R_d and **b** Pr on $Nu_z Re_z^{-\frac{1}{2}}$

- The concentration of Oldroyd-B nanoliquid diminished for enhancing values of C_r and Le.
- The local Nusselt number $(Nu_z Re_z^{-\frac{1}{2}})$ decayed for higher estimations of N_b and N_t.

References

Abel MS, Tawade JV, Nandeppanavar MM (2012) MHD flow and heat transfer for the upper convected Maxwell fluid over a stretching sheet. Meccanica 47:385–393

Ahmed J, Khan M, Ahmad L (2019) Transient thin-film spin-coating flow of chemically reactive and radiative Maxwell nanofluid over a rotating disk. Appl Phys A. https://doi.org/10.1007/s00339-019-2424-0

Alshomrani AS, Irfan M, Salem A, Khan M (2018) Chemically reactive flow and heat transfer of magnetite Oldroyd-B nanofluid subject to stratifications. Appl Nanosci 8:1743–1754

Anjalidevi SP, Kandasamy R (1999) Effects of chemical reaction, heat and mass transfer on laminar flow along a semi-infinite horizontal plate. Heat Mass Transf 35:465–467

Anwar MS, Rasheed A (2017) Simulations of a fractional rate type nanofluid flow with non-integer Caputo time derivatives. Comput Math Appl 74:2485–2502

Choi SUS (1995) Enhancing thermal conductivity of fluids with nanoparticles. ASME Int Mech Eng 66:99–105

Ellahi R (2018) Special issue on recent developments of nanofluids. Appl Sci. https://doi.org/10.3390/app8020192

Haq RU, Rashid I, Khan ZA (2017) Effects of aligned magnetic field and CNTs in two different base fluids over a moving slip surface. J Mol Liq 243:682–688

Haq RU, Soomro FA, Öztop HF, Mekkaoui T (2019) Thermal management of water-based carbon nanotubes enclosed in a partially heated triangular cavity with heated cylindrical obstacle. Int J Heat Mass Transf 131:724–736

Hayat T, Rashid M, Alsaedi A (2017a) MHD convective flow of magnetite-Fe_3O_4 nanoparticles by curved stretching sheet. Result Phys 7:3107–3115

Hayat T, Khan MI, Waqas M, Alsaedi A (2017b) Newtonian heating effect in nanofluid flow by a permeable cylinder. Results Phys 7:256–262

Hayat T, Waqas M, Khan MI, Alsaedi A (2017c) Impacts of constructive and destructive chemical reactions in magnetohydrodynamic (MHD) flow of Jeffrey liquid due to nonlinear radially stretched surface. J Mol Liq 225:302–310

Hayat T, Rashid M, Alsaedi A (2018) Three dimensional radiative flow of magnetite-nanofluid with homogeneous-heterogeneous reactions. Results Phys 8:268–275

Irfan M, Khan M, Khan WA, Ayaz M (2018a) Modern development on the features of magnetic field and heat sink/source in Maxwell nanofluid subject to convective heat transport. Phys Lett A 382:1992–2002

Irfan M, Khan M, Khan WA, Sajid M (2018b) Thermal and solutal stratifications in flow of Oldroyd-B nanofluid with variable conductivity. Appl Phys A. https://doi.org/10.1007/s00339-018-2086-3

Irfan M, Khan M, Khan WA, Sajid M (2019a) Consequence of convective conditions for flow of Oldroyd-B nanofluid by a stretching cylinder. J Braz Soc Mech Sci Eng. https://doi.org/10.1007/s40430-019-1604-3

Irfan M, Khan M, Khan WA (2019b) Impact of Non-uniform heat sink/source and convective condition in radiative heat transfer to Oldroyd-B nanofluid: a revised proposed relation. Phys Lett A 383:376–382

Khan M, Irfan M, Khan WA (2017) Impact of nonlinear thermal radiation and gyrotactic microorganisms on the Magneto-Burgers nanofluid. Int J Mech Sci 130:375–382

Kumar KG, Haq RU, Rudraswamy NG, Gireesha BJ (2017) Effects of mass transfer on MHD three dimensional flow of a Prandtl liquid over a flat plate in the presence of chemical reaction. Results Phys 7:3465–3471

Kumar RVMSSK, Raju CSK, Mahanthesh B, Gireesha BJ, Varma SVK (2018) Chemical reaction effects on nano Carreau liquid flow past a cone and a wedge with Cattaneo-Christov heat flux model. Int J Chem Reactor Eng. https://doi.org/10.1515/ijcre-2017-0108

Mahanthesh B, Gireesha BJ, Gorla RSR, Abbasi FM, Shehzad SA (2016) Numerical solutions for magnetohydrodynamicflow of nanofluid over a bidirectional non-linear stretching surface with prescribed surface heat flux boundary. J Mag Mag Mater 417:189–196

Mahanthesh B, Gireesha BJ, Prasannakumara BC, Kumar PBS (2017a) Magneto-Thermo-Marangoni convective flow of Cu-H_2O nanoliquid past an infinite disk with particle shape and exponential space based heat source effects. Results Phys 7:2990–2996

Mahanthesh B, Mabood F, Gireesha BJ, Gorla RSR (2017b) Effects of chemical reaction and partial slip on the three-dimensional flow of a nanofluid impinging on an exponentially stretching surface. Eur Phys J Plus. https://doi.org/10.1140/epjp/i2017-11389-8

Meghed AM (2013) Variable fluid properties and variable heat flux effects on the flow and heat transfer in a non-Newtonian Maxwell fluid over an unsteady stretching sheet with slip velocity. Chin Phys B 22:094701

Mustafa M, Khan JA, Hayat T, Alsaedi A (2015) Analytical and numerical solutions for axisymmetric flow of nanofluid due to non-linearly stretching sheet. Int J Non-Linear Mech 71:22–29

Rashid M, Hayat T, Alsaedi A (2019) Entropy generation in Darcy–Forchheimer flow of nanofluid with five nanoarticles due to stretching cylinder. Appl Nanosci. https://doi.org/10.1007/s13204-019-00961-2

Rehman FU, Nadeem S, Haq RU (2017) Heat transfer analysis for three-dimensional stagnation-point flow over an exponentially stretching surface. Chin J Phys 55:1552–1560

Sheikholeslami M, Oztop HF (2017) MHD free convection of nanofluid in a cavity with sinusoidal walls by using CVFEM. Chin J Phys 55:2291–2304

Sheikholeslami M, Haq RU, Shafee A, Li Z, Elaraki YG, Tlili I (2019) Heat transfer simulation of heat storage unit with nanoparticles and fins through a heat exchanger. Int J Heat Mass Transf 135:470–478

Sreedevi P, Reddy PS, Chamkha AJ (2017) Heat and mass transfer analysis of nanofluid over linear and non-linear stretching surfaces with thermal radiation and chemical reaction. Powder Technol 315:194–204

Waqas M, Khan MI, Hayat T, Alsaedi A (2017a) Numerical simulation for magneto Carreau nanofluid model with thermal radiation: a revised model. Comput Methods Appl Mech Eng 324:640–653

Waqas M, Khan MI, Hayat T, Alsaedi A (2017b) Stratified flow of an Oldroyd-B nanoliquid with heat generation. Result Phys 7:2489–2496

Zhang C, Zheng L, Zhang X, Chen G (2015) MHD flow and radiation heat transfer of nanofluids in porous media with variable surface heat flux and chemical reaction. Appl Math Model 39:165–181